

*Letter to the Editor***Vibrationally excited vinyl cyanide in Sgr B2(N)****A. Nummelin and P. Bergman**

Onsala Space Observatory, SE-439 92 Onsala, Sweden

Received 18 September 1998 / Accepted 27 November 1998

Abstract. We analyse the excitation of 114 rotational transitions of vinyl cyanide (acrylonitrile), C_2H_3CN , in its ν_{11} and ν_{15} vibrational states, together with 98 transitions in the ground state. The data were taken from the SEST line survey of Sgr B2(N) in the 1.3 mm band. For the lines with energies above 200 K a rotational temperature of 440_{-90}^{+190} K, a C_2H_3CN column density of $5.1_{-2.5}^{+7.2} \times 10^{18}$ cm $^{-2}$, and a source size in the range 0.025–0.037 pc are most consistent with observations. The resulting abundance of C_2H_3CN is about 6×10^{-8} . We argue that the high rotation temperature of the high-energy lines is most likely due to direct radiative excitation through far-infrared emission from hot dust. A Monte-Carlo analysis was applied to the radiative transfer of the lines with upper-state energies below 200 K. A good fit to the intensities of the *a*-type lines is achieved by a model cloud with a fractional C_2H_3CN abundance of 4×10^{-10} . By increasing the abundance to 6×10^{-9} in the outer portion of the cloud also the intensities of the *b*-type lines could be reasonably well fitted. This model is, however, inconsistent with the low intensities of low-energy *a*-type lines observed at longer wavelengths. Hence, we favour a constant C_2H_3CN abundance of 4×10^{-10} in the part of the cloud where the kinetic temperature is below 180 K, and regard the excitation of the intrinsically weak *b*-type lines as anomalous.

Key words: ISM: abundances – ISM: molecules – ISM: individual objects: Sgr B2 – radio lines: ISM

1. Introduction

Vinyl cyanide (acrylonitrile), C_2H_3CN , is a well known interstellar molecule detected through its rotational lines both in molecular clouds (Gardner & Winnewisser 1975) and in dark clouds (Matthews & Sears 1983). It is a planar, near-symmetric ($\kappa = -0.98$) prolate top (symmetry group C_s) with a dominant *a*-type dipole moment ($\mu_a = 3.82$ D, $\mu_b = 0.89$ D; Stolze & Sutter 1985). Vinyl cyanide has 15 normal vibrational modes which can be classified as either symmetric (A') or antisymmetric (A'') with respect to the plane of symmetry of the molecule (Halverson, Stamm, & Whalen 1948;

Cerceau et al. 1985). The lowest-energy vibration in each of these groups is the *b*-type CCN in-plane (ν_{11}) and the *c*-type out-of-plane (ν_{15}) bending modes at 344 K ($\lambda 42 \mu\text{m}$) and 489 K ($\lambda 29 \mu\text{m}$) above the ground state, respectively. Because of the rather low energy of these vibrational states, they can be expected to be significantly populated under interstellar conditions, e.g. in star-forming regions, and Schilke et al. (1997) assigned five lines in their survey of Orion-KL to vibrationally excited C_2H_3CN . There are also other vibrational modes in C_2H_3CN with rather low excitation energies (≥ 980 K) and high band strengths which may be astrophysically significant.

In this Letter, we analyse the excitation of a large number of rotational transitions in the ν_{11} and ν_{15} vibrational states of C_2H_3CN observed towards the hot molecular core Sgr B2(N). The data were taken from our 218–263 GHz spectral line survey of three positions towards the Sgr B2 cloud performed with the 15 m SEST¹, which was described in detail by Nummelin et al. (1998a). Ground state C_2H_3CN was detected in both Sgr B2(N) and Sgr B2(M), but not in Sgr B2(NW), whereas vibrationally excited C_2H_3CN was detected exclusively in Sgr B2(N).

2. Results*2.1. General*

In the SEST survey towards the Sgr B2(N) position² we identified 98 C_2H_3CN rotational lines from the ground vibrational state, 64 lines from the $1\nu_{11}$ state, 45 lines from the $1\nu_{15}$ state, and 5 lines from the $2\nu_{11}$ state. Approximately 25% of the C_2H_3CN flux detected in the 218–263 GHz band is caused by lines in the ν_{11} and ν_{15} states. A sample spectrum from the survey including one of the C_2H_3CN bands is shown in Fig. 1. The integrated line intensities and transition parameters are tabulated by Nummelin et al. (1998a), Table 40.

The majority (77) of the detected ground-state transitions are *a*-type, *R* branch, whereas 21 of the transitions are *b*-type, *Q* and *R* branches. The *a*-type, ground state lines have upper-state energies (E_u) between 145 and 672 K, and the *b*-type

¹ The Swedish–ESO Submillimetre Telescope is operated jointly by ESO and the Swedish National Facility for Radio Astronomy, Onsala Space Observatory, at Chalmers University of Technology.

² $\alpha(1950) = 17^{\text{h}}44^{\text{m}}10.1^{\text{s}}$, $\delta(1950) = -28^{\circ}21'17.0''$

Send offprint requests to: A. Nummelin (albert@oso.chalmers.se)

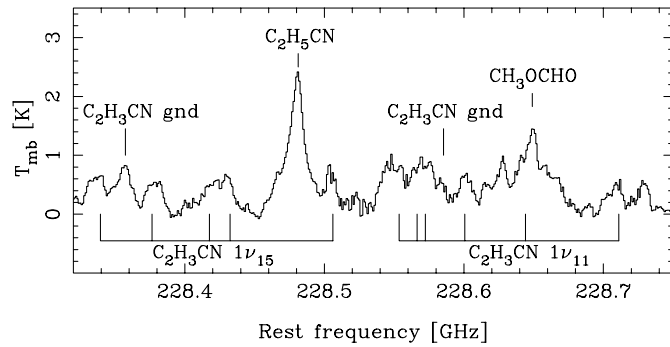


Fig. 1. Sample frequency band from the SEST spectral line survey towards the Sgr B2(N) position, with lines in the C_2H_3CN $J=24 \rightarrow 23$ rotational ladders in the ground state, $1\nu_{11}$, and $1\nu_{15}$ states indicated

lines are in the 22–194 K range. Because of the smaller dipole moment involved, the A -coefficients of the b -type transitions are several times smaller than for the a -type transitions at similar frequencies. The observed vibrationally excited lines are all a -type, R branch, and span 475–1100 K in energy.

The measured centre frequencies of most lines agree within 2–3 MHz with the rest frequencies at an average emission velocity of about 64 km s^{-1} for both the ground-state and vibrationally excited lines. The frequency scatter is somewhat larger for the vibrational lines, which is probably due to their lower intensities. The average velocity width of the C_2H_3CN lines is about 13 km s^{-1} (full width at half maximum, FWHM), without any significant differences between the low-energy lines, the higher-energy ground state lines, and the vibrationally excited lines.

In Fig. 2 we display the data in the rotation diagram format. The data seem to outline two branches with a pronounced break at 180 K. We have applied two different analyses to this data set: The lines with upper-state energies below 200 K were analysed using a Monte-Carlo model, and for the lines above 200 K we derived a column density and rotation temperature using a modified rotation diagram technique. The reason for not applying the Monte-Carlo model to the full data set is the vast number of transitions involved, i.e. computer limitations.

2.2. The low-temperature component

To solve the excitation and radiative transfer of the C_2H_3CN transitions with $E_u < 200 \text{ K}$, we applied a Monte-Carlo technique which included 517 levels below 290 K and approximately 4400 radiative transitions. The method is identical to that described by Bernes (1979), except that a dust continuum component has been added to our model. The model cloud is spherically symmetric and at a distance of 8.5 kpc. The physical parameters throughout the cloud have been set according to the model by Zmuidzinas et al. (1995), except that in our model the cloud has been truncated at an inner radius of 0.05 pc, and at an outer radius of 5 pc. In this range the kinetic temperature, which is equal to the dust temperature, decreases from 180 K to 18 K. As a crude approximation to the C_2H_3CN – H_2 collision rates, we

have adopted the values calculated for the CH_3CN – H_2 system by Green (1986). The fundamental $\Delta K = 0, 3, 6$ CH_3CN – H_2 rates were interpolated so that rates obeying $\Delta K_a = 1, 2, 4, 5$ could be estimated. The collisional rates do not depend on the pseudo-quantum number K_c , since C_2H_3CN has been treated as a symmetric-top molecule. This model of the core of Sgr B2 produces a continuum antenna temperature of approximately 1.6 K, in agreement with observations (Nummelin et al. 1998a). The H_2 column density averaged over a $23''$ beam becomes $2.6 \times 10^{24} \text{ cm}^{-2}$, consistent with the column density derived by Goldsmith, Snell, & Lis (1987), $N(H_2) = 4 \times 10^{24} \text{ cm}^{-2}$, at the same angular resolution.

We found that good agreement with the low-energy data was obtained with a model (denoted model 1) where the fractional abundance $X(C_2H_3CN)$ was dependent on the cloud radius in the following manner. Between $r = 0.05 \text{ pc}$ and 0.6 pc ($50 \text{ K} < T_{\text{kin}} < 180 \text{ K}$) $X(C_2H_3CN) = 4 \times 10^{-10}$, and between $r = 0.6 \text{ pc}$ and 2.5 pc ($25 \text{ K} < T_{\text{kin}} < 50 \text{ K}$) $X(C_2H_3CN) = 6 \times 10^{-9}$. With a uniformly high abundance throughout the cloud, the a -type lines around 150 K become too strong relative to the lower-energy lines. The model line intensities towards the centre of the cloud are rather insensitive to the abundance in the outer cloud, but $X(C_2H_3CN) = 4 \times 10^{-10}$ for $2.5 \text{ pc} < r < 5 \text{ pc}$ ($18 \text{ K} < T_{\text{kin}} < 25 \text{ K}$) is more consistent with the lack of C_2H_3CN emission towards Sgr B2(NW), at $46''$ angular distance from Sgr B2(N) (Nummelin et al. 1998a), although the fit to the data is adequate below 10^{-8} . The C_2H_3CN column density resulting from this model is $6.4 \times 10^{15} \text{ cm}^{-2}$ in a $23''$ beam, and the peak optical depths through the cloud centre are small (< 0.3) in the observed transitions.

However, for $E_u < 145 \text{ K}$ all observed transitions are b -type, and, hence, intrinsically weak. With the abundance of C_2H_3CN set according to model 1, the a -type transitions with high A -coefficients, which occur at 3 mm and longer wavelengths, become far too strong. Comparing with five low-energy (7–28 K) C_2H_3CN lines observed in the Nobeyama line survey of Sgr B2(N) (Ohishi 1998, private communication), these are indeed several times weaker than predicted by model 1. If the fractional abundance of C_2H_3CN is instead kept at 4×10^{-10} throughout the cloud (model 2), satisfactory agreement with data is achieved for the a -type transitions, including the Nobeyama data, whereas the predicted intensities of all the b -type lines are too small compared to data (see Fig. 2). Excessively strong b -type lines of C_2H_3CN and other complex molecules is a well-known problem noted in previous surveys (Turner 1991; Nummelin et al. 1998a). Hence, the excitation of the b -type transitions is considered anomalous, and model 2 is favoured. We have not been able to model this as an effect of high optical depths. The hypothesis of collisional pumping was tried by Turner (1991) without success. Likewise, our results show no indications that such effects could be responsible.

2.3. The high-temperature component

If we assume that the energy level populations can be described by a single rotational temperature T_{rot} , and that there are no

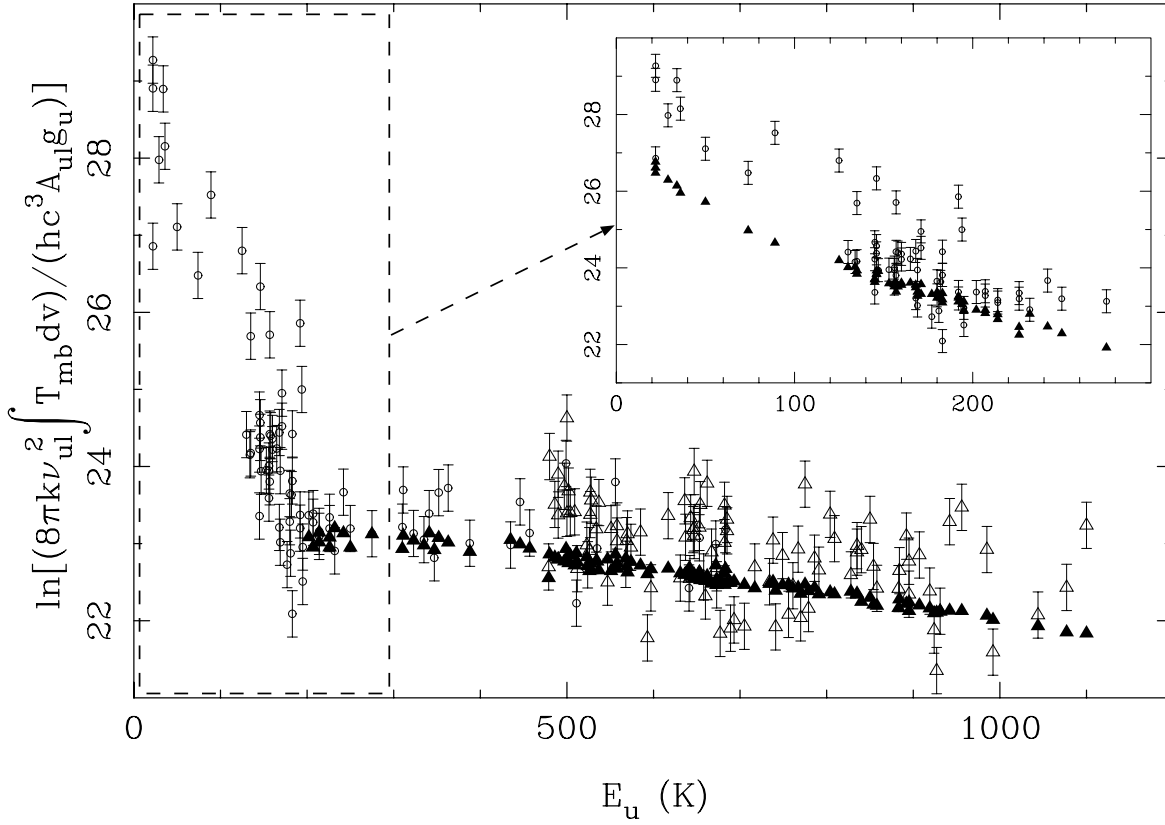


Fig. 2. Rotation diagram of C_2H_3CN , including the lines in the ground state (circles), and in the $1\nu_{11}$, $2\nu_{11}$, and $1\nu_{15}$ vibrational states (open triangles). The error bars indicate 30% uncertainty. Filled triangles indicate predictions by a best-fit model with $T_{\text{rot}} = 440$ K, $N = 5.1 \times 10^{18} \text{ cm}^{-2}$, and a source size of $0.7''$, found by the least- χ^2 procedure described in Sect. 2.3. The expanded diagram shows the observed data points below 300 K (circles), together with the predictions (filled triangles) of the Monte-Carlo analysis (model 2).

physical gradients along the line-of-sight, the antenna temperature of each transition can be calculated through

$$T_A = \eta [J_\nu(T_{\text{rot}}) - J_\nu(T_{\text{bg}})] (1 - e^{-\tau_{ul}}), \quad (1)$$

where η is the fraction of the antenna main-beam area subtended by the source, $J_\nu(T) = (h\nu_{ul}/k)/(e^{h\nu_{ul}/kT} - 1)$, and T_{bg} is the temperature of the background radiation. The optical depth, τ_{ul} , is calculated as

$$\tau_{ul} = \frac{\sqrt{\ln 2}}{4\pi^{3/2}} \frac{c^3 A_{ul} N g_u}{\nu_{ul}^3 Q(T) \Delta v} e^{-E_u/kT} (e^{h\nu_{ul}/kT} - 1),$$

where c is the speed of light, h is Planck's constant, k is Boltzmann's constant, A_{ul} is the Einstein coefficient for spontaneous radiative decay, N is the C_2H_3CN column density, g_u is the statistical weight of the upper state, ν_{ul} is the transition frequency, and Δv is the velocity FWHM of the line. The rotation-vibration partition function, including the ν_{11} and ν_{15} vibrational states, was approximated as

$$Q(T) \approx 5.05 T^{3/2} (1 - e^{-344/T})^{-1} (1 - e^{-489/T})^{-1}.$$

The rotational temperature and C_2H_3CN column density that best reproduce the observed line intensities was defined by the minimum of the reduced χ^2 -value across the two-dimensional (T_{rot}, N) parameter space. Also the parameter uncertainties can be obtained from the χ^2 -values (see Nummelin et al. 1998b).

The rotation temperature and beam-averaged ($23''$) column density that thus best fit the high-energy ($E_u > 200$ K) lines are 570_{-60}^{+80} K and $5.2_{-1.0}^{+1.4} \times 10^{15} \text{ cm}^{-2}$ (1σ error limits), respectively. However, the vibrationally excited emission should, considering the severe excitation requirements and high T_{rot} , be confined to a core region $\ll 23''$. By fitting a T_{rot} and N to the data for a wide range of beam-filling factors we find the following. For $\eta \leq 3 \times 10^{-3}$ the rotational lines start becoming optically thick, which results in a best-fit T_{rot} decreasing with η down to about 420 K (at $\eta \approx 1.2 \times 10^{-3}$). Once the lines are optically thick their intensities are determined by the product of T_{rot} and η , cf. Eq. (1), and T_{rot} therefore increases for $\eta < 1.2 \times 10^{-3}$. Models with $\eta < 10^{-4}$ give poor fits to the data. Under the assumption that the excitation is governed by emission from hot dust (see Sect. 3.1) we may use the relation between dust temperature, radius, and source luminosity by Scoville & Kwan (1976) to put further constraints on η . Beam-filling factors outside the range $1.0_{-0.3}^{+0.5} \times 10^{-3}$, corresponding to a source size range 0.025–0.037 pc, result in inconsistently large ($> 10^7 L_\odot$) luminosities (see Lis & Goldsmith 1990). For this interval we find $T_{\text{rot}} = 440_{-90}^{+190}$ K and $N = 5.1_{-2.5}^{+7.2} \times 10^{18} \text{ cm}^{-2}$, where the error limits include both 1σ statistical errors and parameter variations over the η interval. The line optical depths are typically 0.2–2.5. For comparison, recent high-resolution observations of Sgr B2(M)

have shown that the size of the individual ultra-compact H II-regions is about 10^{-3} pc (De Pree, Goss, & Gaume 1998).

The radial gas density distribution by Zmuidzinas et al. convolved with a $0.7''$ ($\eta = 10^{-3}$) Gaussian implies an H_2 column density of about $8 \times 10^{25} \text{ cm}^{-2}$, which yields $X(C_2H_3CN) = 6 \times 10^{-8}$. We note that this abundance is significantly larger than the abundance derived for the cooler gas, although it of course depends on the uncertain values of the source size and the H_2 column density.

3. Discussion

3.1. Excitation

The A -coefficient for the $1\nu_{11} \rightarrow \text{gnd}$ transition can be estimated from the strength of the $\Delta v = 1$ band reported by Cerceau et al. (1985), and is approximately 0.02 s^{-1} . As an approximation to the collision coefficients we adopt the value for the $27 \mu\text{m } 1\nu_8 \rightarrow \text{gnd}$ band in CH_3CN , $10^{-12} \text{ cm}^3 \text{ s}^{-1}$, reported by Goldsmith et al. (1983). The critical H_2 density for a two-level system is, in the optically thin case, $n_{H_2}^* = A_{ul}/C_{ul}$, where C_{ul} is the collision coefficient. The resulting critical H_2 density for the ν_{11} state becomes $2 \times 10^{10} \text{ cm}^{-3}$, which may be taken as a measure of the high density required for collisional excitation to be important.

If the vibrational states are excited purely by radiation from hot dust, the rotation temperature estimated for the hot component, 440 K, will equal the dust temperature, assuming optically thick dust emission at $29 \mu\text{m}$ and $42 \mu\text{m}$, and that the molecules are fully immersed in the radiation. The large bolometric luminosity of Sgr B2(N), 10^6 – $10^7 L_\odot$ (Lis & Goldsmith 1990), certainly makes far-infrared radiation from hot dust a viable mechanism for population of the ν_{11} and ν_{15} states of C_2H_3CN . As was argued by Goldsmith et al. (1983) for CH_3CN , we favour the explanation that the ν_{11} and ν_{15} states of C_2H_3CN are populated directly by radiation from hot dust at $42 \mu\text{m}$ and $29 \mu\text{m}$, respectively, rather than through collisions, because of the high critical density, and since hot dust is required even in the purely collisional case to heat the gas to sufficiently high kinetic temperature.

We find it less likely that the highly excited C_2H_3CN observed would be residing directly in hot post-shock regions, mainly because of the large column density deduced. For comparison, the shock model by Hollenbach & McKee (1989) for example suggests a column density of post-shock H_2 gas with kinetic temperature of 500 K on the order of 10^{21} cm^{-2} , although a simplistic single-shock model can hardly be directly applied to Sgr B2(N).

As for the anomalously strong b -type transitions, neither high optical depths nor collisional processes seem to provide an explanation. A model including the lowest-lying vibrational

states of C_2H_3CN should be tried in order to try to confirm or disprove the possibility that these lines are affected by radiative processes involving ro-vibrational transitions. However, such an investigation is impossible with our present model due to the large number of transitions involved.

3.2. Abundance

The fractional abundance of C_2H_3CN in Sgr B2(N) derived here, 4×10^{-10} and 6×10^{-8} for the cool and hot component, respectively, can be compared to the abundances observed in the Orion Hot Core, 2×10^{-9} (Blake et al. 1987), and in TMC-1, 3×10^{-10} [Matthews & Sears 1983; assuming $N(H_2) = 10^{22} \text{ cm}^{-2}$]. The homogeneous gas-phase model by Lee, Bettens, & Herbst (1996) does predict abundances as high as $(3\text{--}5) \times 10^{-10}$ at early times (10^5 yr), which accounts for the observed abundances in the cooler gas in Sgr B2(N) and in dark clouds. In their chemical model of the hot cores in Orion, in which C_2H_3CN is a dust-evaporated species, Caselli, Hasegawa, & Herbst (1993) predict an abundance of $(0.2\text{--}1) \times 10^{-8}$, which is in good agreement with Orion data, but somewhat low compared to the abundance in the hot gas in Sgr B2(N).

Acknowledgements. We thank John Black and Åke Hjalmarson for comments on the manuscript, Masatoshi Ohishi for obtaining vinyl cyanide intensities from the NRO survey, and the Swedish Natural Science Research Council (NFR) for financial support.

References

- Bernes, C. 1979, A&A, 73, 67
- Blake, G. A., et al. 1987, ApJ, 315, 621
- Caselli, P., Hasegawa, T. I., Herbst, E. 1993, ApJ, 408, 548
- Cerceau, F., et al. 1985, Icarus, 62, 207
- De Pree, C. G., Goss, W. M., & Gaume, R. A. 1998, ApJ, 500, 847
- Gardner, F. F., & Winnewisser, G. 1975, ApJ, 195, L127
- Goldsmith, P. F., Snell, R. L., & Lis, D. C. 1987, ApJ, 313, L5
- Goldsmith, P. F., et al. 1983, ApJ, 274, 184
- Green, S. 1986, ApJ, 309, 331
- Halverson, F., Stamm, R. F., & Whalen, J. J. 1948, J. Chem. Phys., 16, 808
- Hollenbach, D., & McKee, C. F. 1989, ApJ, 342, 306
- Lee, H.-H., Bettens, R. P. A., & Herbst, E. 1996, A&AS, 119, 111
- Lis, D., & Goldsmith, P. F. 1990, ApJ, 356, 195
- Matthews, H. E., & Sears, T. J. 1983, ApJ, 272, 149
- Nummelin, A., et al. 1998a, ApJS, 117, 427
- Nummelin, A., et al. 1998b, A&A, 337, 275
- Schilke, P., et al. 1997, ApJS, 108, 301
- Scoville, N. Z., & Kwan, J. 1976, ApJ, 206, 718
- Stolze, M., & Sutter, D. H. 1985, Z. Naturforsch., 40a, 998
- Turner, B. E. 1991, ApJS, 76, 617
- Zmuidzinas, J., et al. 1995, ApJ, 447, L125